Electronic Supplementary Information

Propulsion mechanism by electrohydrodynamic (EHD) flow

A highly charged dielectric particle can deform the local electrical field in the vicinity of a conducting electrode. The tangential component of the deformed electric field can, as a consequence, locally drive the induced charges on the electrode and cause an electrohydrodynamic (EHD) flow in an alternating potential. These EHD flows have been previously studied from a fundamental perspective[1] and applied for colloidal assembly[2,3]. More recently, breaking the symmetry of the EHD flow using asymmetric colloidal molecules has also been investigated by Wu and coworkers for locomotion[4–6]. This mechanism is different from the well-known propulsion mechanism driven by induced-charge electro-osmosis (ICEO) where, usually, a metallic patch has to be incorporated in an asymmetric particle[7], although both propulsions are activated in an AC electric field. The inset to Figure S3 schematically illustrates the unbalanced EHD flows for the example of a PS-SiO_2 dimer. The actual directions of the EHD flows at both sides of PS-SiO_2 dimers have been visualized experimentally[4] and the unbalanced EHD flow can propel the dimer with the SiO_2 lobe moving in the front. Here, we fabricate PS-SiO_2 dimers by sCAPA and find the same swimming direction and the same scaling law with the electric field strength (Figure S3). The swimming speed v increases linearly with the square of the field strength E^2, which pinpoints the origin of the driving mechanism on EHD flows, as described by other experimental and modeling studies[1,4]. In particular, the velocity of the electro-hydrodynamic flow is $U_{EHD} \sim C \frac{E^2 \varepsilon \varepsilon_0 \kappa H}{\mu} \frac{K' + \bar{\omega} K''}{1 + \bar{\omega}^2}$, where C is a geometrical factor (e.g. from particle size and shape), E is the applied electrical field strength, $\varepsilon\varepsilon_0$ is the solvent permittivity, κ^{-1} is the Debye length, H is the separation between two electrodes, μ is the viscosity of the medium, $\bar{\omega}$ is the dimensionless frequency ($\bar{\omega} = \omega H/\kappa D$, where D is the ion diffusivity), K' and K'' are real part and imaginary part of the complex polarization coefficient[8], respectively. Both K' and K'' are sensitive to the field frequency ω, the particle radius r, the ion diffusivity D, the Debye length κ^{-1} and the particle surface chemistry, i.e. the zeta potential ζ and the Stern layer conductance σ. This implies that, any asymmetry in zeta potential, Stern layer conductance (both often related to surface composition) and size can lead to an unbalanced EHD flow around the lobes of a colloidal molecule, which further drives net propulsion.

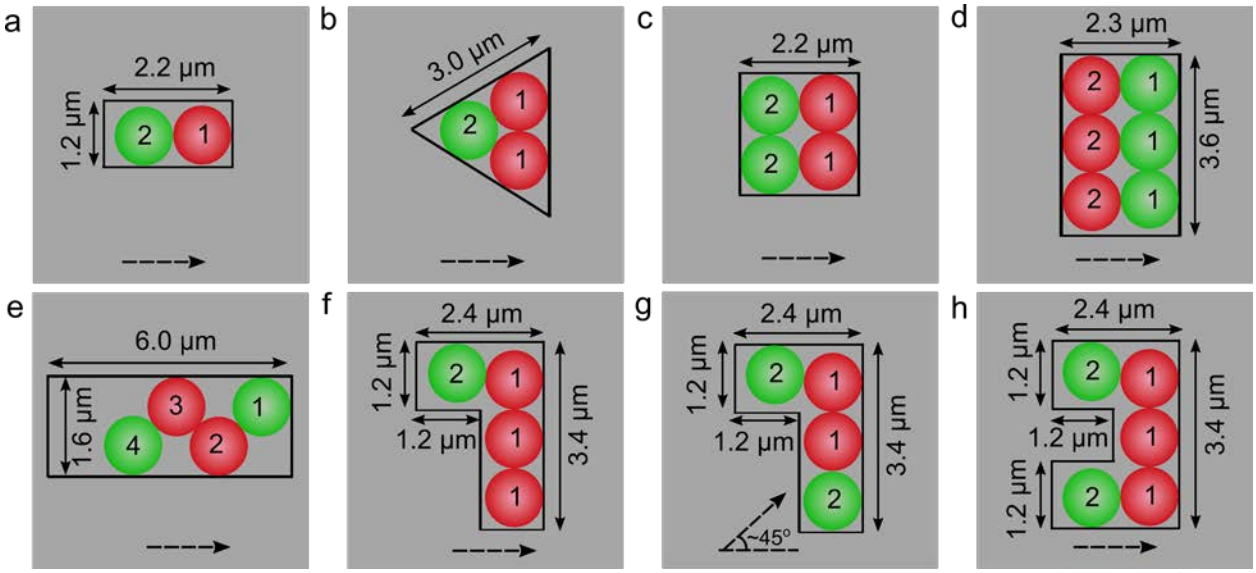

Figure S1. Design and assembly of different active colloidal molecules. (a – h) Schemes showing the lateral dimensions of the traps used, the assembly directions and sequences. All traps have a depth varying between 500 and 550 nm. All particles have a diameter of 1 to 1.1 µm. Dashed arrows indicate the assembly directions. The numbers on the spheres represent the sequence in the assembly, e.g., 1 stands for the first step and 2 for the second step, etc. Spheres in different color stand for different materials. (a – d) Colloidal molecules with different shapes: dumbbells (a), triangles (b), squares (c) and "six-packs" (d) can be assembled sequentially in two steps. (e) A zig-zag colloidal chain can be assembled in four steps by controlling the width of the trap. Tighter traps (trap width close to particle diameter) lead to straighter chains, whereas wider traps lead to colloidal chains with a zig-zag configuration. (f – g) Two types of L-shaped colloidal molecules. (f) The first type can be assembled in two steps, with the assembly direction perpendicular to the long arm of the CM. (g) The second type can also be assembled in two steps, but the assembly direction is turned by 45°, as shown by the dashed arrow. (h) U-shaped colloidal molecules can be assembled in two steps using the trap design shown here.

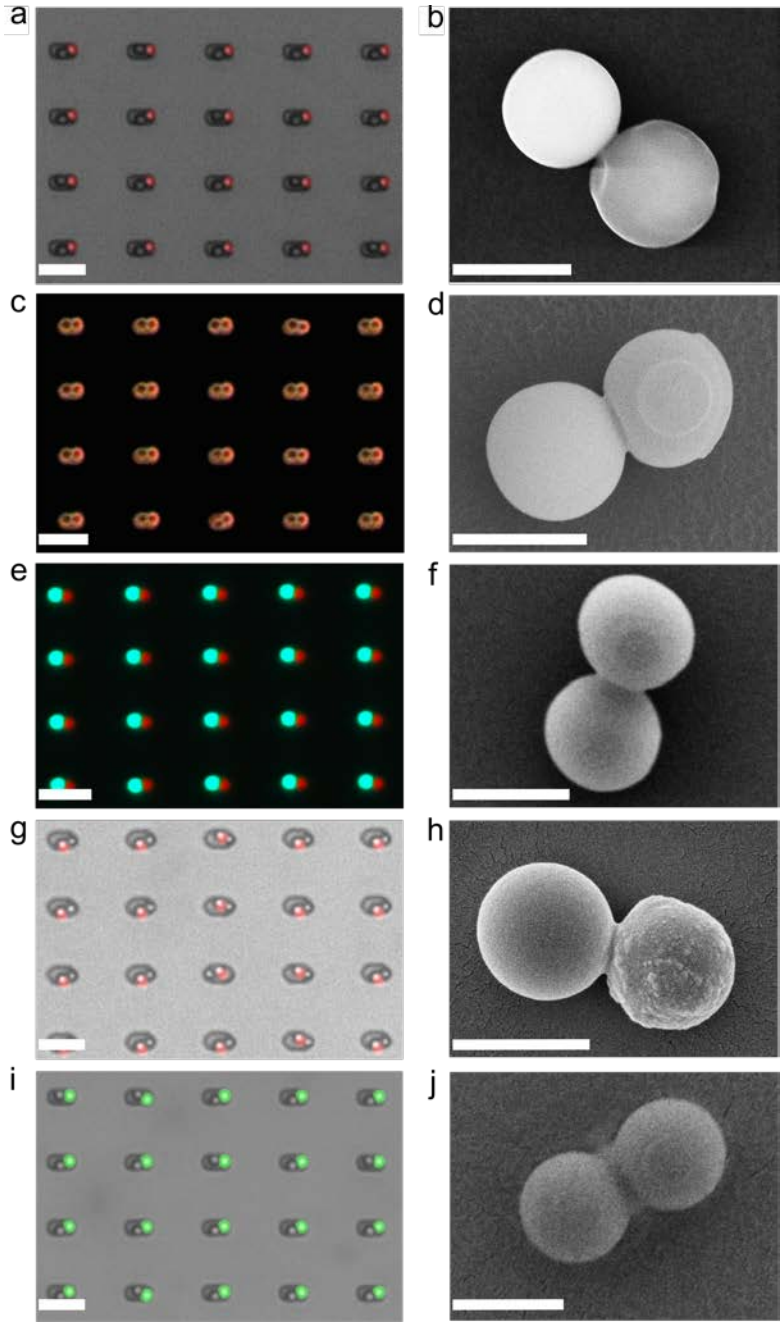

Figure S2. Optical and SEM images of all the dumbbell-like colloidal molecules. (a-b) Overlay of a fluorescence and a bright-field image (a) and SEM image after printing to a silicon substrate (b) for PS/SiO_2 dumbbell. (c-d) Dark-field image (c) and SEM image after printing to a silicon substrate (d) for PS/TiO_2 dumbbell. (e-f) Dual-channel fluorescence image (e) and SEM image after printing to a silicon substrate (f) for PS/PS-NH_2 dumbbell. (g-h) Overlay of a fluorescence and a bright -field image (g) and SEM image after printing to a silicon substrate (h) for PS/SiO_2-Mag dumbbell. (i-j) Overlay of a fluorescence and a bright-field image (i) and SEM image after printing to a silicon substrate (j) for PS-NH_2/SiO_2 dumbbell. Scale bars: 5 µm (a, c, e, g, i) and 1 µm (b, d, f, h, j).

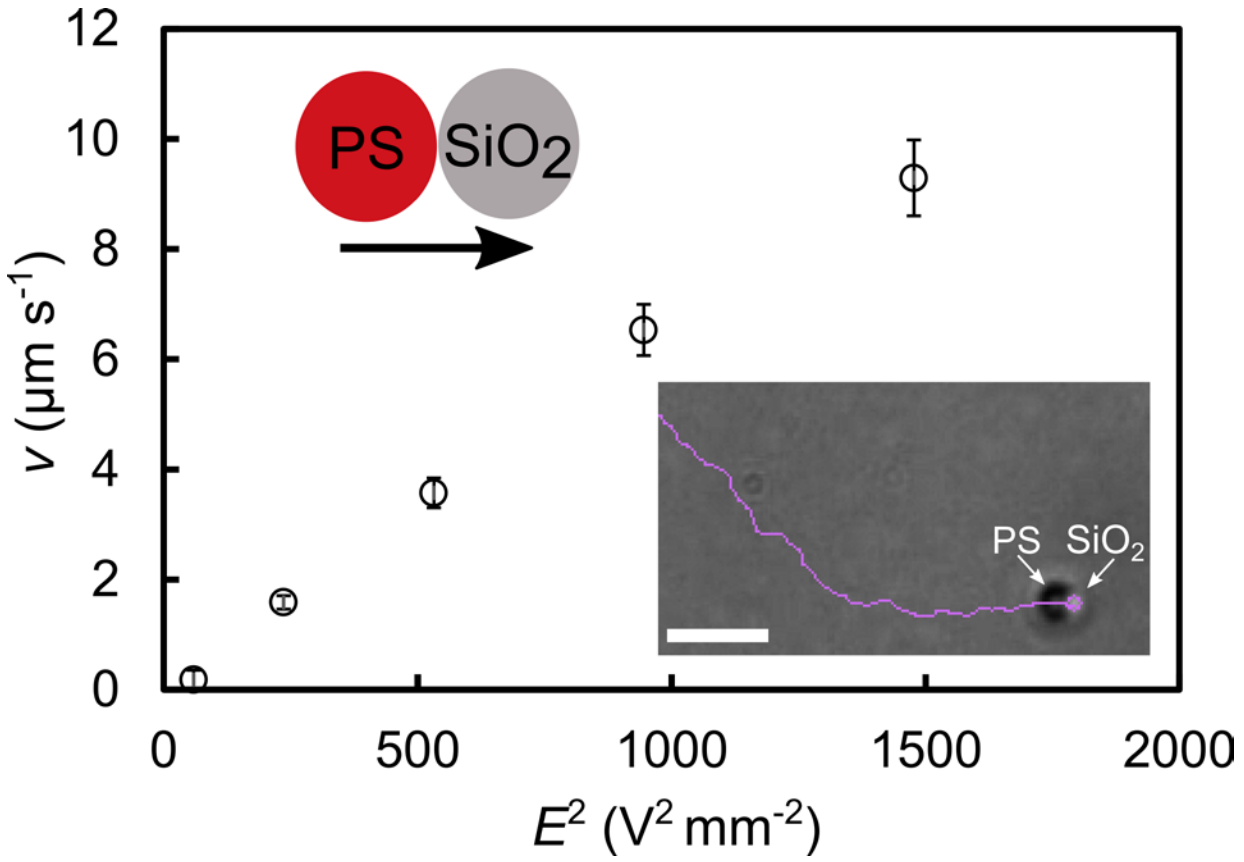

Figure S3. Swimming speed *v* plotted versus the square of the electrical field strength E^2 for PS/SiO_2 dumbbells. *v* increases linearly with E^2. The bright-field image (inset) shows a PS/SiO_2 dumbbell with its trajectory. The scheme indicates the propulsion direction. Scale bar: 5 μm.

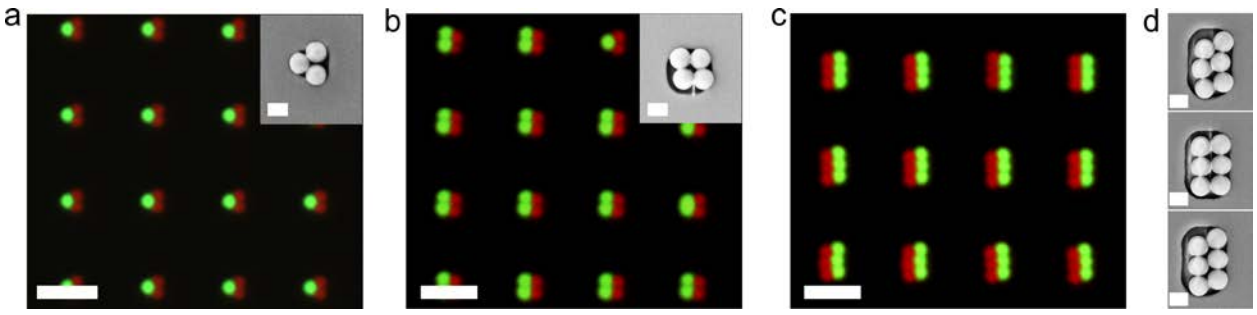

Figure S4. Fluorescence and SEM images for triangle (a), square (b) and six-pack-like (c) colloidal molecules. (d) The structure of six-pack-like CMs can vary depending on the trap used, which accounts for the larger error bar present in Figure 2b in the main text. Scale bars: 5 μm (a, b, c), 1 μm in the insets of (a, b) and in (d).

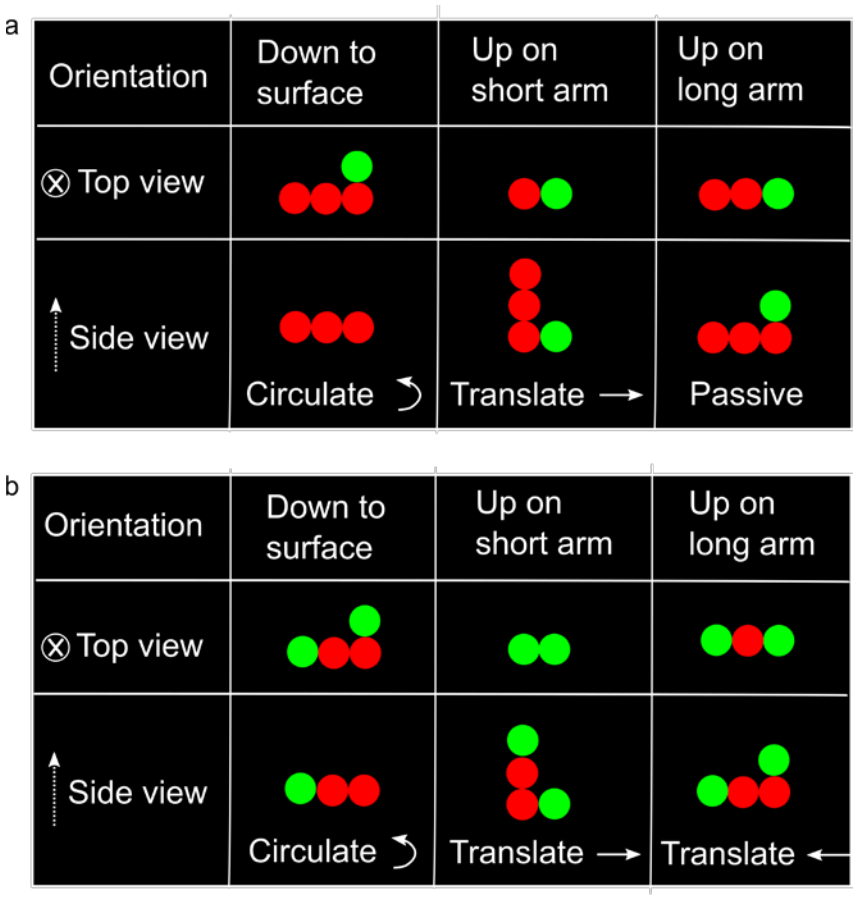

Figure S5. Comparison of the types of motion for two types of L-shaped active colloidal molecules at different orientations, without (a) and with (b) a green particle at the end of the long arm (red: PS particles; green: PS-NH_2 particles). (a) L-shaped active colloidal molecules without a green particle at the long arm perform circular motion while lying flat and translate while standing up on the short arm, but do not exhibit any active motion while standing up on the long arm because there is no asymmetric electro-osmotic flow parallel to the substrate. (b) L-shaped active colloidal molecules with a green particle also perform circular motion while lying flat, but translate while standing up, both on the short and on the long arm.

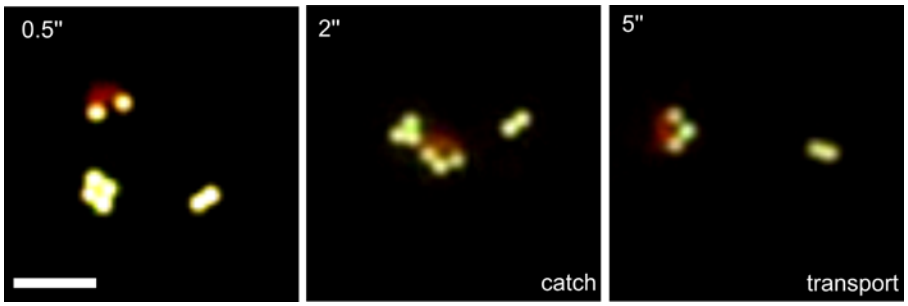

Figure S6. Transport of a PS-NH_2 target particle by the U-shaped colloidal microswimmer on a patterned electrode. A U-shaped CM picks up a PS-NH_2 (green) particle and transports it, as shown by the time series of fluorescence images (corresponding Movie S13). Scale bar: 5 µm.

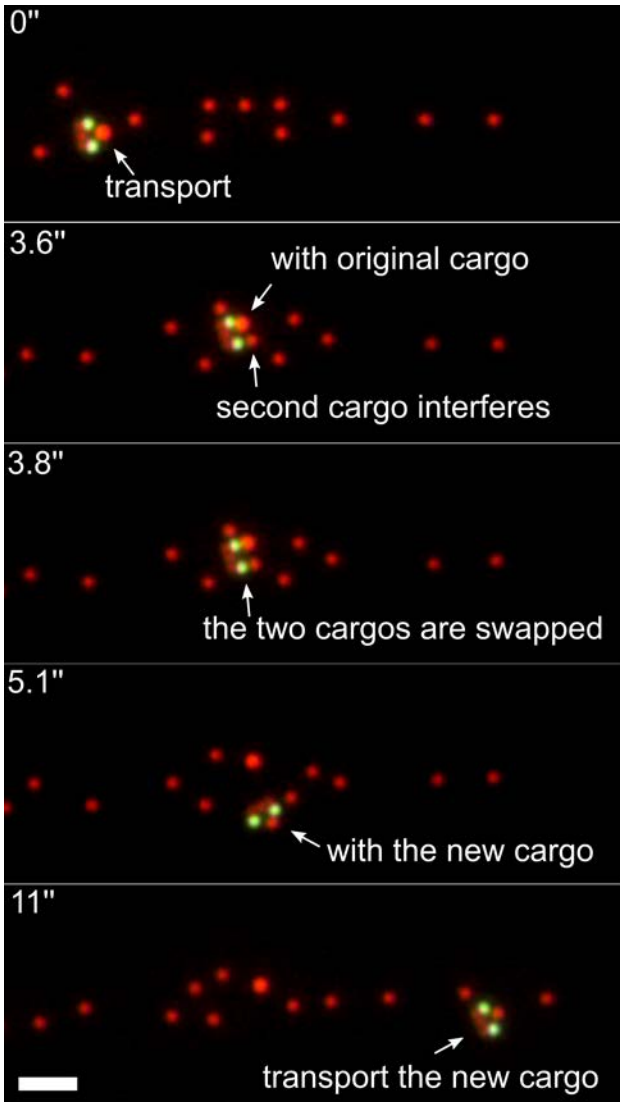

Figure S7. Cargo swap by a U-shaped colloidal microswimmer in a crowded environment. Initially, the U-shaped CM is transporting its cargo particle through a crowded environment of other PS particles. At the time of 3.6'', another particle (red, PS) is close enough to hinder the motion of the U-shaped CM, in particular the motion on one arm. This disturbance leads to the situation in which the cargo and the second particle are in close proximity to the CM and become equally probable to be picked up (see the time at 3.8''). In the example selected, the cargo is swapped, and the U-shaped CM travels on with the new cargo particle (see frames at 5.1" and 11"). Scale bar: 5 μm.

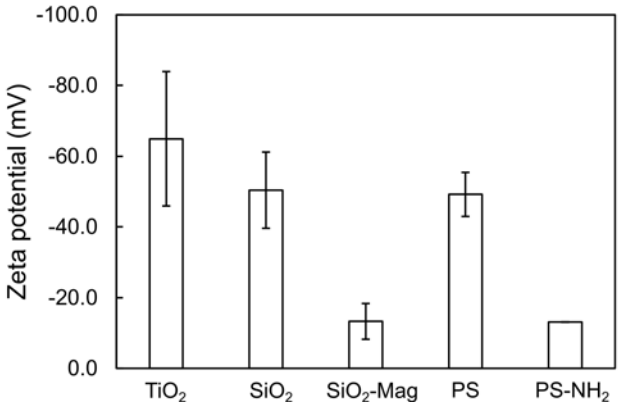

Figure S8. Zeta potential measured for different single particles used in this study.

Movie S1. An actuated and self-propelling, dumbbell-like colloidal molecule. The movie was captured by dual-channel fluorescence microscopy at 10 fps, with an applied AC electrical field at 1.3 kHz, 25 V (peak to peak voltage) and a spacer of 220 μm.

Movie S2. An actuated and self-propelling, square-like colloidal molecule. The movie was captured by dual-channel fluorescence microscopy at 10 fps, with an applied AC electrical field at 1.3 kHz, 25 V (peak to peak voltage) and a spacer of 220 μm.

Movie S3. An actuated and self-propelling, six-pack-like colloidal molecule. The movie was captured by dual-channel fluorescence microscopy at 10 fps, with an applied AC electrical field at 1.3 kHz, 22 V (peak to peak voltage) and a spacer of 245 μm.

Movie S4. An actuated and self-propelling, L-shaped colloidal molecule. The movie was captured by dual-channel fluorescence microscopy at 10 fps, with an applied AC electrical field at 1kHz, 26 V (peak to peak voltage) and a spacer of 250μm.

Movie S5. An actuated and self-propelling, U-shaped colloidal molecule. The movie was captured by dual-channel fluorescence microscopy at 10 fps, with an applied AC electrical field at 1 kHz, 20 V (peak to peak voltage) and a spacer of 240 μm.

Movie S6. An actuated and rotating, zigzag-like colloidal molecule. The movie was captured by dual-channel fluorescence microscopy at 7 fps, with an applied AC electrical field at 1 kHz, 24 V (peak to peak voltage) and a spacer of 230 μm.

Movie S7. A reconfigurable, L-shaped colloidal molecule, switching from circular to translational (standing on the short arm) motion. The movie was captured by dual-channel fluorescence microscopy at 10 fps, with an applied AC electrical field (1 kHz to 1 MHz back to 1 kHz), 20 V (peak to peak voltage) and a spacer of 230 μm.

Movie S8. A reconfigurable, L-shaped colloidal molecule, switching from circular to translational (standing on the long arm) motion. The movie was captured by dual-channel fluorescence microscopy at 10 fps, with an applied AC electrical field (1 kHz to 1 MHz back to 1 kHz), 20 V (peak to peak voltage) and a spacer of 230 μm.

Movie S9. An actuated, dumbbell-like colloidal molecule swimming along the straight patterned electrode. The movie was captured by dual-channel fluorescence microscopy at 10 fps, with an applied AC electrical field at 1 kHz, 20 V (peak to peak voltage) and a spacer of 230 μm.

Movie S10. A failed pick up by a square-like active colloidal molecule. The movie was captured by dual-channel fluorescence microscopy at 10 fps, with an applied AC electrical field at 1 kHz, 20 V (peak to peak voltage) and a spacer of 300 μm.

Movie S11. A failed pick up and transport by a six-pack-like active colloidal molecule. The movie was captured by dual-channel fluorescence microscopy at 10 fps, with an applied AC electrical field at 1 kHz, 20 V (peak to peak voltage) and a spacer of 300 μm.

Movie S12. A complete and successful pick up (red particle), transport and release by a U-shaped active colloidal molecule. The movie was captured by dual-channel fluorescence microscopy at 10 fps, with an applied AC electrical field at 1 kHz, 20 V (peak to peak voltage) and a spacer of 300 μm.

Movie S13. A successful pick up (green particle) and transport by a U-shaped active colloidal molecule. The movie was captured by dual-channel fluorescence microscopy at 10 fps, with an applied AC electrical field at 1 kHz, 20 V (peak to peak voltage) and a spacer of 290 μm.

Movie S14. A U-shaped active colloidal molecule swimming in a crowded environment after picking up a cargo. The movie was captured by dual-channel fluorescence microscopy at 10 fps, with an applied AC electrical field at 1 kHz, 20 V (peak to peak voltage) and a spacer of 290 μm.

Movie S15. A U-shaped active colloidal molecule swapping cargo during transportation. The movie was captured by dual-channel fluorescence microscopy at 10 fps, with an applied AC electrical field at 1 kHz, 20 V (peak to peak voltage) and a spacer of 300 μm.

References

1 W. D. RISTENPART, I. A. AKSAY and D. A. SAVILLE, *J. Fluid Mech.*, 2007, **575**, 83–109.
2 M. Trau, D. A. Saville and I. A. Aksay, *Langmuir*, 1997, **13**, 6375–6381.
3 R. C. Hayward, D. A. Saville and I. A. Aksay, *Nature*, 2000, **404**, 56–59.
4 F. Ma, X. Yang, H. Zhao and N. Wu, *Phys. Rev. Lett.*, 2015, **115**, 208302.
5 S. Wang, F. Ma, H. Zhao and N. Wu, *ACS Appl. Mater. Interfaces*, 2014, **6**, 4560–4569.
6 F. Ma, S. Wang, D. T. Wu and N. Wu, *Proc. Natl. Acad. Sci.*, 2015, **112**, 6307–6312.
7 T. . SQUIRES and M. . BAZANT, *J. Fluid Mech.*, 2006, **560**, 65–101.
8 H. Zhou, M. A. Preston, R. D. Tilton and L. R. White, *J. Colloid Interface Sci.*, 2005, **285**, 845–856.